The EMBO Journal Vol.18 No.22 pp.6211–6220, 1999

Membrane raft microdomains mediate front–rear polarity in migrating cells

Santos Mañes[1], Emilia Mira, Concepción Gómez-Moutón, Rosa Ana Lacalle, Patrick Keller[2], Juan Pablo Labrador and Carlos Martínez-A

Department of Immunology and Oncology, Centro Nacional de Biotecnología, Consejo Superior de Investigaciones Científicas, Universidad Autónoma de Madrid, Campus de Cantoblanco, E-28049 Madrid, Spain and [2]Cell Biology Programme, European Molecular Biology Laboratory, Meyerhofstrasse 1, D-69117 Heidelberg, Germany

[1]Corresponding author
e-mail: smanes@cnb.uam.es

S.Mañes and E.Mira contributed equally to this work

The acquisition of spatial and functional asymmetry between the rear and the front of the cell is a necessary step for cell chemotaxis. Insulin-like growth factor-I (IGF-I) stimulation of the human adenocarcinoma MCF-7 induces a polarized phenotype characterized by asymmetrical CCR5 chemokine receptor redistribution to the leading cell edge. CCR5 associates with membrane raft microdomains, and its polarization parallels redistribution of raft molecules, including the raft-associated ganglioside GM1, glycosylphosphatidylinositol-anchored green fluorescent protein and ephrinB1, to the leading edge. The non-raft proteins transferrin receptor and a mutant ephrinB1 are distributed homogeneously in migrating MCF-7 cells, supporting the raft localization requirement for polarization. IGF-I stimulation of cholesterol-depleted cells induces projection of multiple pseudopodia over the entire cell periphery, indicating that raft disruption specifically affects the acquisition of cell polarity, but not IGF-I-induced protrusion activity. Cholesterol depletion inhibits MCF-7 chemotaxis, which is restored by replenishing cholesterol. Our results indicate that initial segregation between raft and non-raft membrane proteins mediates the necessary redistribution of specialized molecules for cell migration.

Keywords: chemokine receptor/chemotaxis/leading edge/lipid rafts/polarization

Introduction

Cell chemotaxis requires the acquisition and maintenance of both spatial and functional asymmetry (polarization) between initially equivalent cell parts. In diapedesing cells, this asymmetry develops between two opposite cell edges: one becomes the leading edge, exhibiting protrusion, and the other becomes the rear edge, undergoing retraction (Lauffenburger and Horwitz, 1996). The acquisition of front–rear polarity is controlled by external directional signals (Zigmond, 1974) that generate a series of repeated excitation and adaptation events. Molecular rearrangement can hence ensue, leading to the cellular spatial asymmetries involved in migration, such as integrin–cytoskeleton linkage (Schmidt *et al*., 1993) as well as forward redistribution of integrin adhesion receptors (Lawson and Maxfield, 1995) and of chemosensory receptors (Sullivan *et al*., 1984).

It has been suggested that asymmetrical membrane distribution may result in an apparent enrichment of chemoattractant receptors at the leading edge, although these receptors are not actively accumulated at this site during chemotaxis (Servant *et al*., 1999). This asymmetry has been observed for different chemoattractant receptors (Walter and Marasco, 1984; Schmitt and Bultmann, 1990; McKay *et al*., 1991), including several chemokine receptors such as CCR2, CCR5 and CXCR4 (Nieto *et al*., 1997; Vicente-Manzanares *et al*., 1998). Chemokine receptor polarization in leukocytes correlates with the acquisition of a migrating phenotype and appears to be independent of the polarization-inducing agent used (McKay *et al*., 1991; Nieto *et al*., 1997). Asymmetrical chemoattractant receptor distribution is thus the conclusive reflection of complex mechanisms that establish and maintain functionally specialized domains in the plasma membrane and cytoplasm during cell migration.

Whereas there are a number of reports on the role of different receptors and signaling molecules activated during the chemotactic response, the signals determining the specific distribution of proteins to one or the other cell pole remain cryptic. Membrane raft microdomains have been proposed as platforms for the selective delivery of membrane proteins to specialized cell surfaces in polarized neurons and epithelial cells (Ledesma *et al*., 1989, 1999; Dotti and Simons, 1990; Simons and Wandinger-Ness, 1990; Simons and Ikonen, 1997). According to this model, specific membrane proteins cluster with glycosphingolipids and cholesterol-enriched membrane rafts in the *trans*-Golgi network (TGN), leading to protein–lipid complexes [detergent-insoluble glycosphingolipid–cholesterol-enriched complexes (DIGs)], which are insoluble after treatment with non-ionic detergents such as Triton X-100 (Brown and Rose, 1992). In non-polarized cells such as BHK, CHO or 3T3 fibroblasts, several membrane proteins are also delivered with glycosphingolipids in vesicular carriers from the TGN to the cell surface (Müsch *et al*., 1996; Yoshimori *et al*., 1996; Keller and Simons, 1998). Since these protein–lipid complexes are conserved on the surface of living cells (Friedrichson and Kurzchalia, 1998; Varma and Mayor, 1998), it would be reasonable to believe that the initial raft and non-raft protein segregation may have functional significance once the cells have a polarized phenotype. Accordingly, recent evidence suggests that membrane compartmentalization between rafts and non-rafts is

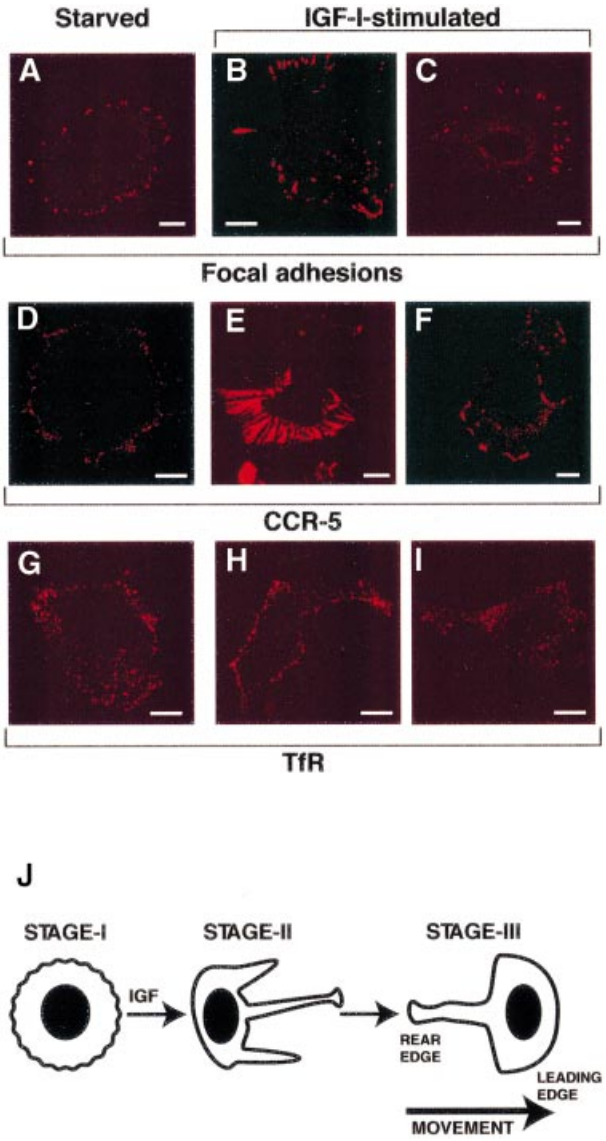

Fig. 1. IGF-I stimulation induces a polarized phenotype. Unstimulated (starved) or IGF-I-stimulated cells were stained for immunofluorescence with an anti-paxillin antibody (**A**–**C**) to visualize focal adhesions, or with an anti-CCR5 antibody (**D**–**F**). TfR distribution (**G**–**I**) was analyzed by incubating the cells with rhodamine-labeled human transferrin as described in Materials and methods. Bar, 10 μm. (**J**) Summary of the phenotypes found in MCF-7 cells.

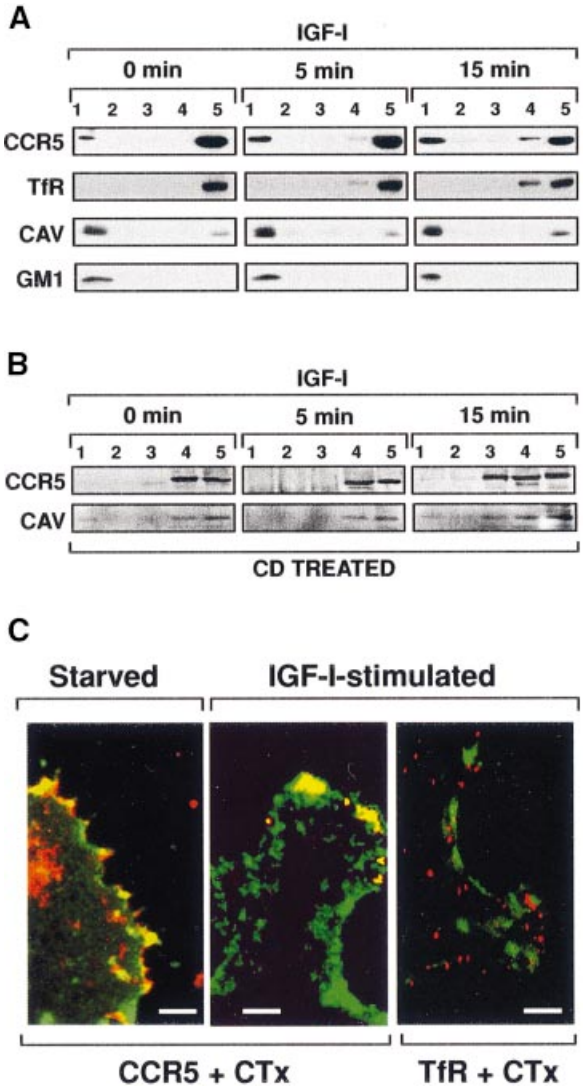

Fig. 2. CCR5 is found constitutively in rafts. (**A**) Increased stability of CCR5 in DIGs after IGF-I stimulation. Serum-starved MCF-7 cells were incubated with IGF-I (30 min at 4°C). Cells were then washed twice with DMEM containing 0.1% BSA and transferred to 37°C for the indicated times. After incubation, cells were Triton X-100 extracted and fractionated in Optiprep flotation gradients. Fractions were collected from the top to the bottom of the gradient and analyzed by Western blotting with antibodies to CCR5, to the transferrin receptor (TfR), to caveolin (cav), and with biotin-labeled CTx B-subunit to detect the raft-associated ganglioside GM1. Data shown are representative of four independent experiments. (**B**) Methyl-β-cyclodextrin (CD) treatment abolished association of CCR5 with membrane microdomains. Serum-starved MCF-7 cells were treated with 10 mM CD (30 min at 37°C) before incubation with IGF-I as described above. Triton X-100 extracts were fractionated and analyzed by Western blotting with antibodies to CCR5 and caveolin (cav). (**C**) CCR5 co-localizes with GM1 in intact cells. Serum-starved or IGF-I-stimulated MCF-7 cells were fixed, stained with FITC–CTx B-subunit (CTx, green) and either CCR5 or TfR antibodies, as indicated, followed by a Cy3-labeled second antibody (red), and analyzed by confocal microscopy. Amplification of a representative area is shown. Bar, 5 μm.

required for efficient T-cell activation (Montixi *et al*., 1998; Xavier *et al*., 1998), and that T-lymphocyte co-stimulation is mediated by reorganization of membrane raft microdomains (Viola *et al*., 1999).

Here we studied the mechanisms used to acquire front–rear polarity in migrating tumor cells, using the human breast adenocarcinoma MCF-7 cell line as a model system. MCF-7 cells migrate in response to insulin-like growth factor-I (IGF-I), but not in the absence of stimulus (Doerr and Jones, 1996). The IGF-I chemotactic effect on MCF-7 cells is independent of *de novo* protein synthesis, and involves an increase in integrin-mediated cell adhesion and the activation of the type-1 IGF receptor (IGF-1R)-mediated signaling pathways necessary for the integrin deactivation process (Mañes *et al*., 1999; Mira *et al*., 1999).

We report that IGF-I induces clustering and asymmetrical distribution of CCR5 to the leading cell edge. In addition, IGF-I-induced CCR5 polarization correlates with distribution of the raft-associated ganglioside GM1 to the same cell pole. CCR5 associates with DIGs in unstimulated cells and IGF-I stimulation increases the amount of CCR5 in the Triton X-100-insoluble fractions. We further show

polarization of other raft-associated proteins to the leading edge of migrating cells, although they have no functional role in chemotaxis. Finally, membrane cholesterol depletion specifically impedes IGF-I-induced polarization and chemotaxis, suggesting that protein–lipid interactions in membrane raft microdomains mediate acquisition of the front–rear polarity necessary for cell migration.

Results

IGF-I induces a polarized migrating phenotype

IGF-I induces polarized morphology in MCF-7 cells, as well as changes in cell surface distribution of the chemokine receptor CCR5. We used the criterion that focal adhesion formation occurs preferentially at the cell front (Izzard and Lochner, 1980; Regen and Horwitz, 1992) to determine unequivocally the leading edge of migrating MCF-7 cells. Unstimulated MCF-7 cells show a rounded morphology on which focal adhesions and CCR5 are uniformly distributed (Figure 1A and D). Shortly after IGF-I stimulation (5–10 min), cell spreading increases and the cell issues a variable number of pseudopodia and lamellipodia, which have a large number of focal adhesions and show strong CCR5 staining (Figure 1B and E). One extension eventually predominates and forms the leading edge. At longer stimulation times, both the leading edge, rich in focal contacts, and a trailing tail with few or no focal adhesions are clearly distinguished (Figure 1C). Asymmetrical CCR5 distribution is also evident when a polarized phenotype is attained, with CCR5 staining located mainly at the leading cell edge (Figure 1F). Other membrane receptors such as the transferrin receptor (TfR) are distributed homogeneously, independent of cell phenotype (Figure 1G–I), as observed using rhodamine-labeled human transferrin. Similar results were obtained after lateral cross-linking with anti-TfR antibodies (data not shown), indicating that neither antibody staining nor fixation affect membrane protein distribution. In summary, IGF-I-induced MCF-7 phenotypic changes were classified in three stages (Figure 1J). Stage I is characterized by rounded, unstimulated cells, stage II by increased cell spreading and the start of pseudopod and lamellipodium protrusion, and stage III by cells showing a migrating phenotype with a well-differentiated leading edge and a trailing tail.

The CCR5 chemokine receptor is constitutively associated with DIGs

To comprehend better the molecular mechanisms of asymmetrical CCR5 distribution in IGF-I-polarized MCF-7 cells, we analyzed whether this receptor is localized in membrane rafts. Triton X-100-insoluble membrane raft proteins can be identified by their ability to float in density flotation gradients as DIGs (Brown and Rose, 1992); this property clearly distinguishes them from the insoluble complexes formed by cytoskeleton association. Fractionation of untreated and IGF-I-stimulated MCF-7 cells showed that CCR5 was present in DIGs (Figure 2A). The CCR5 present in the lightest fraction of unstimulated cells represents 11–18% of total CCR5, as determined by densitometric analysis. IGF-I treatment promotes an increase in the amount of CCR5 in the insoluble fraction, increasing to 45–53% and 55–62% of the total CCR5 after 5 and 15 min of stimulation, respectively. Co-purification of the raft protein caveolin and the GM1 lipid in DIGs, and the full solubilization of non-raft proteins such as the TfR, confirm the quality of the preparation. MCF-7 cells were treated with methyl-β-cyclodextrin (CD), a drug that disrupts rafts by removing cholesterol from the membrane, leading to solubilization of raft-associated proteins (Scheiffele *et al*., 1997; Keller and Simons, 1998). CD treatment significantly increased CCR5 solubility in both unstimulated and IGF-I-stimulated cells (Figure 2B). After incubation with fetal calf serum (FCS), which restores membrane rafts (Friedrichson and Kurzchalia, 1998), CD-treated MCF-7 cells partially recover CCR5, as well as raft marker caveolin insolubility (data not shown).

To assess further the results obtained in flotation gradients, we studied CCR5–raft association in intact cells. The ganglioside GM1, which is detected specifically with the cholera toxin B-subunit (CTx) (Schon and Freire, 1989), was used as a raft lipid marker. CTx is pentavalent for GM1, causing the formation of clusters of five GM1 molecules, but not a large GM1 lattice (Merrit *et al*., 1994). Double immunofluorescence analysis with anti-CCR5 antibodies and CTx showed extensive co-localization of both molecules in unstimulated and IGF-I-treated cells (Figure 2C). These data thus concur with those obtained in flotation gradients and support CCR5 association with lipid rafts in the MCF-7 cell membrane. Conversely, clustered TfR detected by patching with anti-TfR-specific antibodies are totally excluded from GM1 patches, as expected (Harder *et al*., 1998).

IGF-1R associates transiently with DIGs following IGF-I stimulation

We next analyzed whether the IGF-1R associates with DIGs in MCF-7 cells. Flotation experiments with serum-starved MCF-7 cells showed that the IGF-1R is present mainly in soluble gradient fractions, but becomes insoluble shortly after IGF-I stimulation (Figure 3A). In unstimulated MCF-7 cells, there is a small amount of the IGF-1R in the lighter gradient fractions, possibly due to autocrine IGF-1R stimulation in this cell line (Rohlik *et al*., 1987). IGF-1R insolubility after IGF-I stimulation correlates with the appearance of the phosphatidylinositol-3-kinase (PI-3K) p85 subunit, one of the earliest substrates activated by the IGF-1R, in the lighter fractions of the gradient. Our results thus show that IGF-1R activation leads to its transient association with DIGs, as also reported for the T-cell receptor in lymphocytes (Montixi *et al*., 1998; Xavier *et al*., 1998).

IGF-1R association to membrane microdomains was also analyzed in intact cells. In serum-starved MCF-7 cells, IGF-1R shows a weak, diffuse cell surface distribution (data not shown). Lateral cross-linking with specific antibodies causes redistribution of plasma membrane elements, which tend to form patches on the cell surface (Spiegel *et al*., 1984; Harder *et al*., 1998). Co-patching experiments using anti-IGF-1R antibody and CTx showed little or no overlap between IGF-1R and GM1 in unstimulated MCF-7 cells (Figure 3B). IGF-I stimulation of MCF-7 causes discrete aggregations of the IGF-1R, as detected with an anti-IGF-I antibody. This antibody recognizes IGF-I–IGF-1R complexes (Mañes *et al*., 1997),

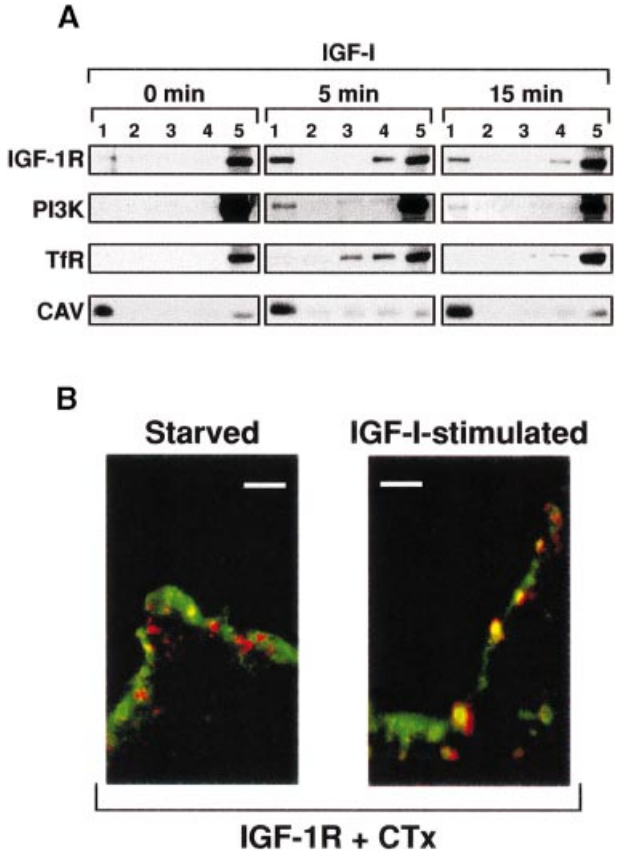

Fig. 3. Activated IGF-1R associates transiently with rafts. (**A**) IGF-I stimulation recruits IGF-1R into DIGs. Serum-starved MCF-7 cells were incubated with IGF-I (30 min at 4°C) as described in Figure 2. Fractions were collected from the top to the bottom of Optiprep flotation gradients after Triton X-100 extraction, and analyzed by Western blotting with antibodies against the IGF-1R β-subunit (IGF-1R), the PI-3K p85 subunit, TfR or caveolin (cav). Results are representative of three independent experiments. (**B**) IGF-1R associates with rafts in intact cells. In serum-starved MCF-7 cells, co-patching is shown using FITC–CTx (green) and an antibody to the IGF-1R α-subunit, followed by Cy3-conjugated second antibody (red). MCF-7 cells were stimulated for 5 min with IGF-I, fixed, stained with FITC–CTx to visualize GM1 (green), and with an anti-IGF-I antibody that binds to the IGF-I–IGF-1R complex, followed by Cy3-second antibody (red). Bar, 5 μm.

permitting specific recognition of growth-factor-activated IGF-1R molecules. Using this anti-IGF-I antibody and CTx, partial overlap of the IGF-1R and GM1 staining was observed after IGF-I stimulation (Figure 3B). Similar results were obtained using an anti-IGF-1R antibody (data not shown).

Asymmetrical GM1 staining in migrating cells

Since CCR5 is distributed asymmetrically during IGF-I-induced cell migration, we examined whether GM1 might have a similar asymmetrical cell membrane distribution. Following IGF-I stimulation, CCR5 staining is concentrated mainly in the growing pseudopodia and in lamellipodia of vitronectin-attached MCF-7 cells (Figure 4A–D). Although GM1 asymmetry is less marked than that observed for CCR5, CTx staining also demonstrates preferential GM1 distribution to these growing structures, as compared with the rest of the cell body. Moreover, in fully polarized MCF-7 cells, CTx labeling detects large GM1 patches in the plasma membrane corresponding to or in close proximity to the leading edge, where staining overlaps with that of CCR5. The trailing tail of the migrating cell is devoid of GM1 labeling (Figure 4E–H). In contrast to GM1, IGF-1R labeling is randomly distributed on the cell surface (Figure 4I–L), similar to that found for the TfR (see Figure 1I). Statistical analysis of a representative number of cells showing homogeneous or asymmetrical distribution of each component is presented in Table I. These data suggest that raft-associated proteins or lipids, such as CCR5 and GM1, are distributed preferentially to the leading edge in migrating MCF-7 cells; membrane receptors not associated with rafts, such as the TfR, or that are transiently associated with these membrane subdomains, such as the IGF-1R, are not segregated and show homogeneous distribution.

Raft association is necessary for protein redistribution to the cell leading edge

We next examined whether any protein associated to membrane raft microdomains would also be redistributed as a consequence of cell polarization. For this, we expressed glycosylphosphatidylinositol-anchored green fluorescence protein (GPI-GFP) in MCF-7 cells. Proteins anchored to the outer leaflet of the cell membrane via a GPI moiety are enriched in the DIG fraction (Brown and Rose, 1992). Accordingly, the GFP-GPI protein is detergent insoluble when overexpressed in MCF-7 cells (Figure 5A); conversely, the non-tagged GFP is soluble in these cells (data not shown). Immunofluorescence analysis showed redistribution of the membrane-anchored GFP-GPI as a consequence of cell polarization (Figure 5B). Whereas GFP-GPI shows uniform membrane distribution in serum-starved cells, the GFP-GPI labeling is concentrated at the leading edge in cells with a migrating phenotype. Quantitative analyses indicated that 82% of the polarized GFP-GPI-transfected cells showed a preferential leading edge distribution of the labeling (Figure 5C).

To address further the role of raft association as a mediator in asymmetrical protein distribution during cell migration, the pattern of overexpressed wild-type ephrinB1 (GFP-ephrinB1wt) or of a C-terminal deletion mutant (GFP-ephrinB1ΔC) was analyzed by immunofluorescence. When overexpressed in MCF-7 cells, a large amount of ephrinB1wt is associated with rafts, whereas ephrinB1ΔC is not (Figure 5A), as reported for other cell lines (Brückner *et al.*, 1999). In serum-starved MCF-7 cells, ephrinB1wt and ephrinB1ΔC are homogeneously distributed on the plasma membrane (Figure 5B). In cells with a polarized phenotype, however, ephrinB1wt patches are concentrated mainly at the cell front, whereas ephrinB1ΔC still shows homogeneous distribution of the GFP patches.

Membrane rafts mediate front–rear polarity required for cell migration

Collectively, the preceding results suggest that membrane protein association with raft microdomains may be an important requirement for their apparent asymmetrical distribution during cell migration. This interpretation predicts that a reduction in membrane cholesterol would inhibit membrane protein asymmetry. MCF-7 cells were treated with CD for 30 min; CD was then removed and IGF-I-induced polarization analyzed. CD-induced choles-

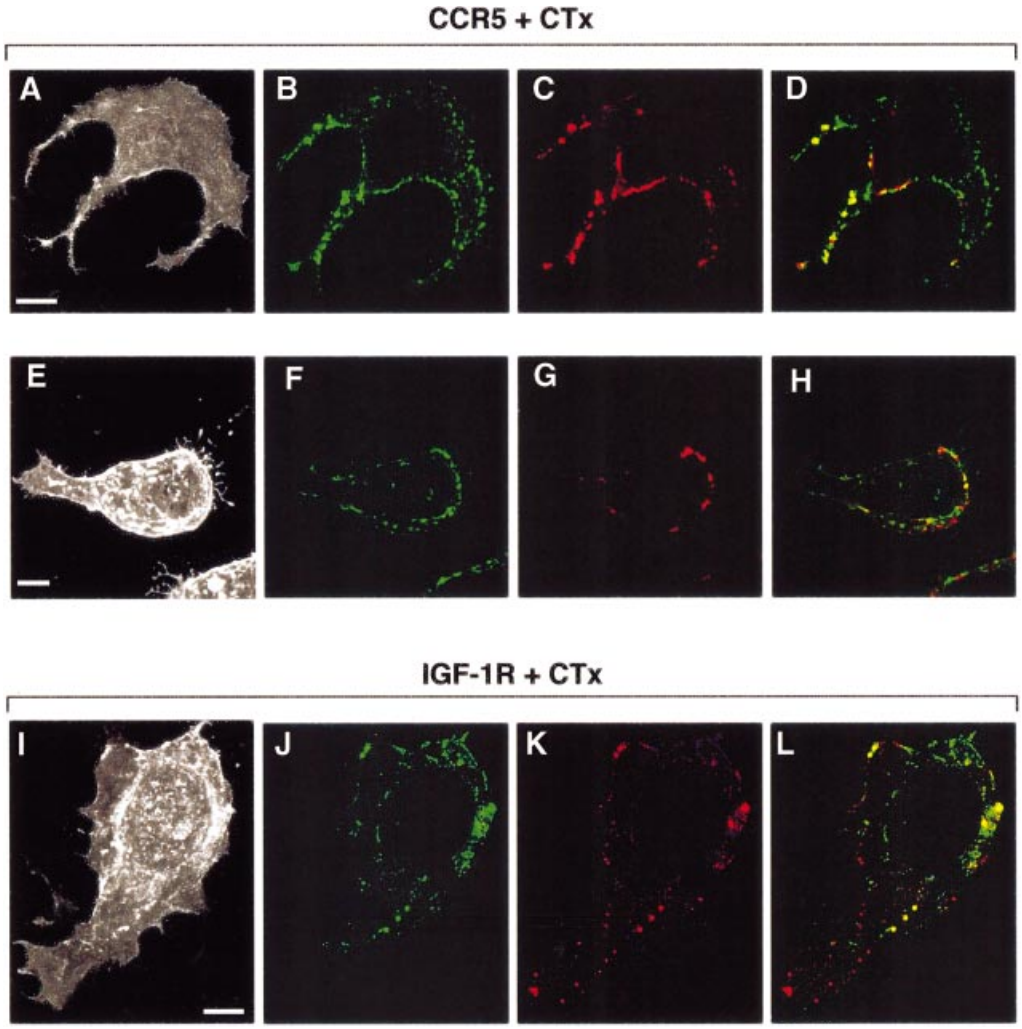

Fig. 4. Membrane rafts are preferentially located at the leading edge of migrating MCF-7 cells. (**A**–**H**) IGF-I-stimulated cells were fixed, then incubated at 4°C with FITC–CTx (green) and CCR5 antibody, followed by Cy3-conjugated secondary antibody (red). The distribution of GM1 (B, F), CCR5 (C, G), and the merging of both signals (D, H) are shown. To visualize cell shape (A, E), laser power for both green and red channels was saturated and the eight sections taken were projected onto one another. In this way, the tail of the cell, devoid of both CCR5 and GM1 labeling, can be visualized. Protruding filopodia clearly identify the leading edge. (**I**–**L**) IGF-I-stimulated MCF-7 cells were incubated with FITC–CTx (green) and an anti-IGF-1R, followed by a Cy3-labeled second antibody (red). Cell shape was recorded as indicated above. The cell in this figure is representative of the vast majority of cells recorded in independent experiments. Bar, 10 μm.

Table I. Asymmetrical distribution of raft-associated markers

Membrane marker	Number of cells[a]			
	Stage I		Stage III	
	Homogeneous	Asymmetrical	Homogeneous	Asymmetrical
CCR5	80/85 (94%)	5/85 (6%)	10/50 (20%)	40/50 (80%)
GM1	90/90 (100%)	0/90 (0%)	27/66 (41%)	39/66 (59%)
TfR	90/90 (100%)	0/90 (0%)	34/40 (85%)	6/40 (15%)
IGF-1R	30/30 (100%)	0/30 (0%)	24/25 (96%)	1/25 (4%)

[a]Cells from stages I and III were recorded and fluorescence scan analysis of a representative confocal section was performed. The number of cells with homogeneous or asymmetrical distribution of the corresponding marker is indicated with respect to the total number of cells recorded. The percentage is indicated in parentheses.

terol depletion was controlled using plasma membrane cholesterol staining with filipin III (data not shown). This short CD treatment neither affects MCF-7 cell survival nor modifies the morphology of unstimulated cells (Figure 6A). Depletion of plasma membrane cholesterol, however, reduces the number of cells that show a migrating phenotype after IGF-I stimulation (Figure 6A). Approximately 20–30% of the untreated cells acquire a polarized cell shape after IGF-I stimulation, whereas only 1–2% of the CD-treated cells show this morphology. Replenishment of plasma membrane cholesterol by incubating CD-treated cells with free cholesterol (Simons *et al.*, 1998) restores

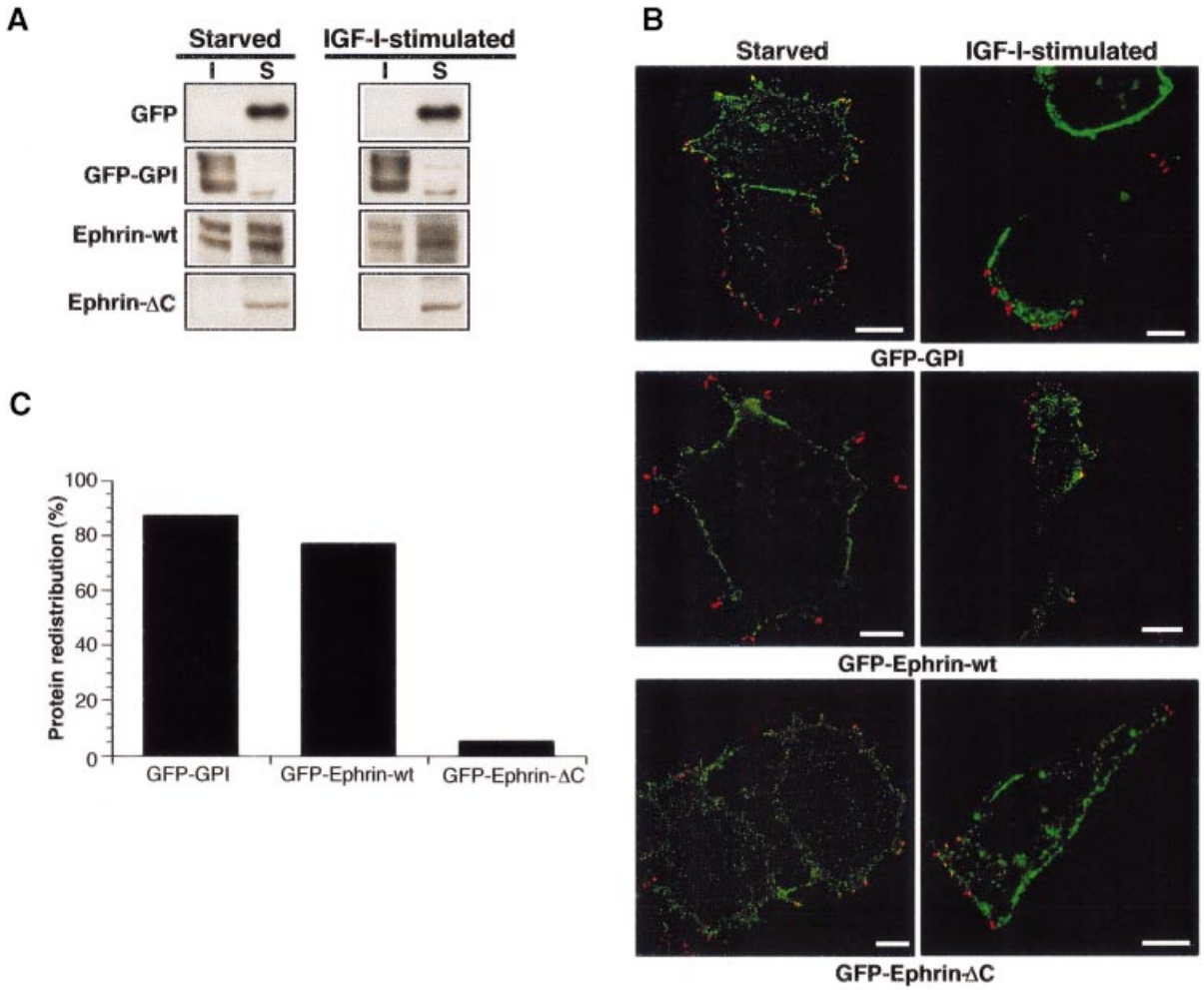

Fig. 5. Raft association is a requisite for preferential redistribution of membrane proteins at the leading cell edge. (**A**) MCF-7 cells were transiently transfected with GFP, GFP-GPI, ephrinB1wt-GFP or the mutant ephrinB1ΔC-GFP, as indicated, and unstimulated or IGF-I-stimulated cells were Triton X-100 extracted and fractionated in Optiprep flotation gradients. Fractions were collected from the top to the bottom of the gradient and analyzed by Western blotting with antibodies to GFP. Only the first, corresponding to insoluble proteins (I), and the last fractions, corresponding to soluble proteins (S), are shown. (**B**) Transfected cells as in (A) were analyzed by immunofluorescence. Panels show fluorescence corresponding to paxillin (red) and GFP (green) for unstimulated or IGF-I-stimulated transfected cells, as indicated. For better visualization, lateral cross-linking of the ephrinB1wt and ephrinB1ΔC was performed using an anti-HA polyclonal antibody before paxillin staining. Bar, 10 μm. (**C**) The proportion of cells showing asymmetrical distribution was calculated by direct counting (n = 50–60) of transfected cells with a polarized phenotype.

the percentage of cells with a migrating phenotype. In addition, IGF-I stimulation of CD-treated cells promotes the extension of a variable number of pseudopodia around the entire cell periphery. This isotropic protrusion of pseudopodia contrasts with that observed in non-CD-treated or cholesterol-replenished cells, in which pseudopodium protrusion is observed from only one cell edge. This indicates that acquisition of the polarized phenotype is specifically impaired in CD-treated cells, although these cells retain other chemoattractant-induced activities such as pseudopodium protrusion. Furthermore, CD-treated MCF-7 cells have reduced chemotaxis in response to IGF-I (Figure 6B), indicating that membrane raft integrity is necessary for directed cell movement. Cholesterol replenishment restores IGF-I-induced MCF-7 chemotaxis; CD treatment does not, however, inhibit IGF-1R-mediated early signaling, such as IGF-1R β-subunit autophosphorylation and IRS-1 recruitment (Figure 7). Collectively, these results indicate that raft integrity is a requisite for acquisition of the front–rear polarity necessary for IGF-I-induced migration.

Discussion

Several lines of evidence presented here suggest that segregation between raft and non-raft proteins in unstimulated cells is a pivotal factor in distributing specialized molecules to specific locations during cell migration. First, raft-associated membrane proteins or lipids are preferentially located at the leading edge following cell-induced polarization; conversely, proteins not located in rafts show a homogeneous distribution over the cell surface. The asymmetrical redistribution of GFP-GPI protein indicates that any raft-associated membrane protein will be routed to the leading edge and, therefore, this asymmetry is not restricted to molecules with functional significance in cell motility or signaling. Secondly, modification of proteins in such a way that they do not associate with rafts inhibits their asymmetrical redistribution in migrating cells. Whereas the raft-associated ephrinB1wt protein preferentially decorates the leading edge, the non-raft-associated mutant ephrinB1ΔC is distributed homogeneously in the plasma membrane of polarized cells.

Thirdly, disruption of rafts by chemical depletion of membrane cholesterol impedes cell polarization and inhibits cell chemotaxis, which may be restored by replenishing membrane cholesterol. These results indicate that raft integrity is required for the acquisition of front–rear polarity and, consequently, for cell motility. Collectively, our findings suggest that the IGF-1R engages all the signaling machinery necessary to induce cell polarization using the lipid microdomains as platforms.

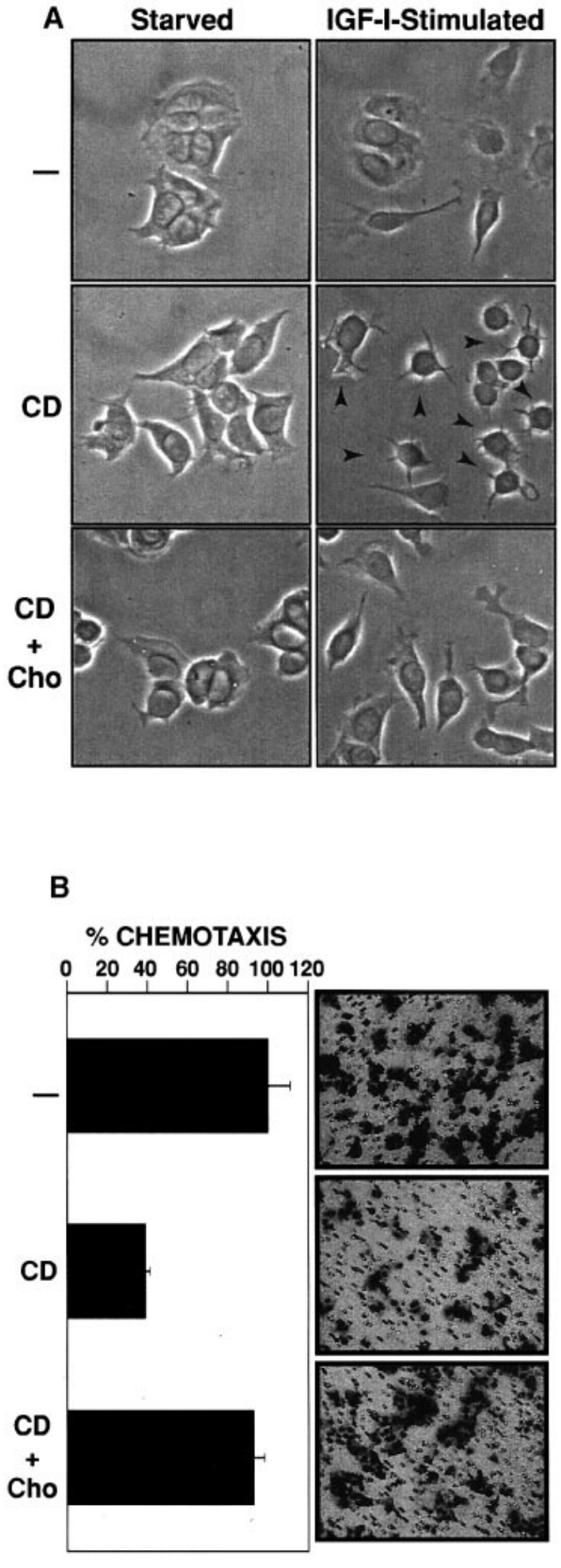

Fig. 6. Membrane rafts mediate the front–rear polarity required for cell chemotaxis. (**A**) Membrane cholesterol depletion impairs cell polarization. Panels show phase-contrast images of untreated, CD-treated and cholesterol-replenished MCF-7 cells after IGF-I stimulation or serum starvation, as indicated. Arrowheads indicate cells with isotropic pseudopodia extension. (**B**) Raft disruption decreases cell migration. Detached cells were incubated (30 min at 37°C) in serum-free medium with 10 mM CD, washed to remove CD, and seeded in the upper chamber of vitronectin-coated transwells. For cholesterol replenishment (CD + Cho), CD-treated cells were incubated for 30 min in medium containing free cholesterol (30 min at 37°C), washed to remove cholesterol, and seeded on vitronectin-coated transwells. Chemotaxis assays were performed using IGF-I as a chemoattractant. IGF-I-induced migration in non-CD-treated cells was considered as 100%. After hematoxylin–eosin staining, a representative field of the transmigrating cells was selected for each treatment and the quantification data are shown.

Membrane raft microdomains are not static elements in plasma membrane organization; on the contrary, they participate in the dynamic regulation of signaling (Simons and Ikonen, 1997). Membrane rafts at steady state are small and highly dispersed, and GM1 staining is accordingly sparse and ill-defined in unstimulated MCF-7 cells. IGF-I–IGF-1R interaction promotes activation of the receptor and its association with rafts, where it recruits signaling proteins such as the p85 subunit of PI-3K. IGF-1R aggregation is concomitant with activation, and IGF-I stimulation may thus trigger the clustering of membrane rafts, which coalesce thereafter into large domains. These patches are clearly visible in cells that have begun to emit pseudopodia. The increase in CCR5 in the light fractions of the flotation gradients following IGF-I stimulation may thus be the consequence of enhanced raft stability induced by IGF-1R clustering. Cross-linking of raft-associated proteins increases the amount of these proteins in the Triton X-100-insoluble membrane fraction without affecting non-raft proteins (Harder *et al*., 1998).

Our results thus support IGF-I regulation of raft dynamics, although identification of the mechanism by which the membrane raft microdomains are directed to the leading edge requires future investigation. The possibility that proteins clustered in rafts migrate to the leading edge on the plane of the plasma membrane cannot be ruled out. Nonetheless, the asymmetrical raft distribution may also occur via a specific, directed transcytotic pathway for membrane rafts. An increasing body of evidence suggests the existence of a polarized endocytotic cycle in the extension of the migrating cell front (reviewed in Bretscher and Aguado-Velasco, 1998). It is thus conceivable that raft redistribution to the migrating cell leading edge may be a consequence of the bulk-flow transport of membrane to this cell pole**.** Nevertheless, the fact that non-raft-associated membrane proteins, such as the TfR, IGF-1R and the ephrinB1ΔC mutant, do not show asymmetrical redistribution in polarized MCF-7 cells ruled out this possibility. Our results thus contradict those showing preferential delivery of endocytosed TfR at the leading edge of migrating fibroblasts (Hopkins *et al*., 1994). A possible explanation for this discrepancy is that both raft and non-raft proteins are delivered to the leading edge due

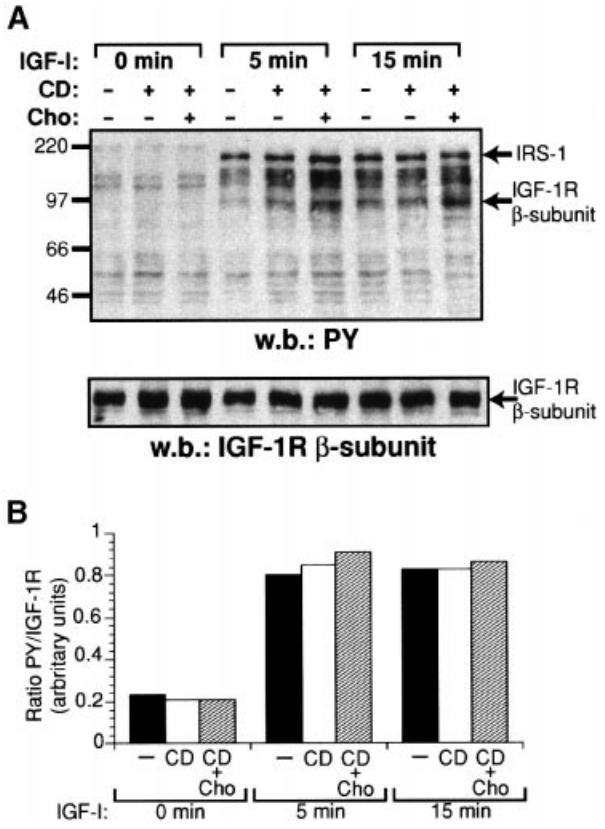

Fig. 7. IGF-1R-dependent early signaling is not impaired by CD treatment. (**A**) Untreated, CD-treated and cholesterol-replenished MCF-7 cells, as in Figure 6, were serum starved, then left untreated or stimulated with IGF-I for different time periods. Equal amounts of cell lysates were resolved in SDS–PAGE. Western blots were hybridized sequentially with specific anti-phosphotyrosine (PY) and anti-IGF-1R β-subunit antibodies. Arrows indicate the band corresponding to the IGF-1R β-subunit and to IRS-1. (**B**) Western blots were digitalized and the 98 kDa band corresponding to the IGF-1R β-subunit was analyzed by densitometry. The ratio of the densitometric signals for the anti-IGF-1R β-subunit and the anti-PY for the same band is represented for each treatment condition.

to membrane flow during migration but only raft-associated proteins are 'retained' at the cell front, whereas TfR and other non-raft-associated proteins are actively transported to the trailing tail by a capping phenomenon (Taylor *et al*., 1971). The actin cytoskeleton reduces lateral mobility of CD44-containing rafts, constraining CD44 patches in the basolateral membrane of epithelial cells (Oliferenko *et al*., 1999). A link between the actin cytoskeleton and rafts has been also suggested in T cells (Harder and Simons, 1999).

The functional role of asymmetrical raft redistribution should also be considered. Based on the experiments shown here, we propose that membrane rafts mediate the acquisition of front–rear polarity in migrating cells. Chemical depletion of membrane cholesterol produces impaired cell polarization induced by IGF-I, although early IGF-1R-mediated signaling events are not affected by CD treatment. An important observation is that the vast majority of cells with reduced cholesterol levels show isotropic protrusion activity. Compared with untreated cells, which show clear anisotropy with pseudopodium emission in only one cell edge, CD-treated cells extend pseudopodia over the entire cell surface. In chemoattractant-induced cell movement, one pseudopodium becomes dominant while others are suppressed; this dominant pseudopodium is stabilized as the leading edge lamellipodium. The process of selection, generation and propagation of a leading edge lamellipodium from a group of random pseudopodia is poorly understood, but may involve stabilization of filaments or active suppression once a leading edge lamellipodium is established (Bailly *et al*., 1998). Our results therefore suggest that although IGF-I is able to induce pseudopodial protrusion in CD-treated cells, the integrity of membrane raft microdomains is necessary for the location-specific induction of the protruding activity or, conversely, for the site specificity of pseudopodial suppression. The impairment in the acquisition of the polarized phenotype following raft disruption may explain the inhibition of IGF-I-induced chemotaxis after membrane cholesterol depletion, and may be analogous to the inactivation of the Cdc42 guanosine triphosphatase effect in the polarization of embryonic fibroblasts (Nobes and Hall, 1999) and T cells (Stowers *et al*., 1995; Allen *et al*., 1998). In addition, the localization of Cdc42 in the caveolae-enriched membrane of endothelial cells has recently been reported (Gingras *et al*., 1998).

A final question is the physiological significance of the raft redistribution described here. Since CCR5 associates with rafts, asymmetrical raft distribution could be considered a mechanism to localize a cell guidance system preferentially at the leading edge. There is nonetheless controversy over whether or not chemoattractant receptors accumulate at the leading edge of migrating cells. Whereas initial studies in fixed neutrophils and T cells indicated clustering of the chemoattractant receptors at the leading edge (Sullivan *et al*., 1984; McKay *et al*., 1991; Nieto *et al*., 1997), recent evidence in living amoebae and neutrophils suggests that these receptors are evenly distributed in cells engaged in chemotaxis (Xiao *et al*., 1997; Servant *et al*., 1999). Our data clearly show asymmetrical staining for CCR5 and other raft-associated proteins; asymmetrical raft redistribution may therefore represent a mechanism that amplifies the detection of chemotactic signals. Cells can detect a front-to-back concentration difference as low as 1% (Zigmond, 1977). Amplification of this asymmetry may occur at the receptor level or downstream, involving the recruitment and/or activation of chemotactic signaling molecules in discrete plasma membrane regions. In amoebae, activation of signaling molecules during chemotaxis occurs within a very defined region of the plasma membrane at the leading edge (Parent *et al*., 1998; Meili *et al*., 1999). Several examples have provided functional evidence that clustering of raft-associated proteins may trigger local signal transduction events (Stauffer and Meyer, 1997). It may thus be postulated that induction of raft redistribution at the leading edge of migrating cells by chemoattractants may have functional significance as a mechanism to locally activate signaling pathways essential for motility and chemotaxis.

Materials and methods

Cell culture and materials

MCF-7 human breast carcinoma cells from the American Type Culture Collection (ATCC; Manassas, VA) were maintained in MEM with 10% FCS, penicillin, streptomycin, L-glutamine, sodium pyruvate and non-essential amino acids. Cells were transfected using Lipofectamine Plus (Gibco-BRL, Gaithersburg, MD) according to the manufacturer's instructions. For immunofluorescence analysis, cells were trypsinized 1 day

later and plated on vitronectin-coated 8-well-chamber glass slides (Nunc, Naperville, IL).

Recombinant human IGF-I was provided by Pharmacia & Upjohn (Stockholm, Sweden). Vitronectin was purchased from Collaborative Biomedical (Bedford, MA). Surfact-Amps X-100 containing 10% Triton X-100 was from Pierce (Rockford, IL). Optiprep gradient medium was from Nycomed Pharma (Oslo, Norway), and CD, water-soluble cholesterol, filipin III, bovine serum albumin (BSA), peroxidase-conjugated streptavidin, and biotin- and fluorescein isothiocyanate (FITC)-labeled CTx B subunit were from Sigma (St Louis, MO).

Antibodies and expression constructs

The anti-CCR5 monoclonal antibody (mAb) used in Western blotting was kindly provided by Dr M.Mellado (DIO/CNB, Madrid, Spain), a CCR5 mAb (Mab182; R&D Systems, Minneapolis, MN) was used for immunocytochemistry analysis, and the anti-TfR mAb used in Western blotting was from Zymed Labs (South San Francisco, CA). Polyclonal anti-caveolin-1 and anti-IGF-1R β-subunit antibodies were from Santa Cruz (Santa Cruz, CA), anti-paxillin mAb from Transduction Laboratories (Lexington, KY) and peroxidase-conjugated anti-phosphotyrosine (PY) antibody 4G10 was from Upstate Biotechnology (Lake Placid, NY). Monoclonal and anti-IGF-1R α-subunit (α-IR3) and anti-TfR antibodies used in immunocytochemical analysis were from Oncogene Research (Cambridge, MA). The monoclonal anti-IGF-I antibody (clone KM5A1) recognizing the IGF-I–IGF-1R complexes has been described before (Mañes *et al*., 1997). Peroxidase- or Cy3-labeled secondary antibodies were from Dako (Glostrup, Denmark) or Jackson ImmunoResearch (West Grove, PA), respectively. Polyclonal anti-HA for ephrinB1 patching experiments was purchased from Babco (Richmond, CA).

GFP-ephrinB1wt (pJP136) and GFP-ephrinB1ΔC (pJP139) constructs were described previously (Brückner *et al*., 1999). The GFP-GPI construct will be described elsewhere (Keller *et al.*, manuscript in preparation). To study the distribution of these overexpressed proteins on the plasma membrane of migrating MCF-7 cells, transfected cells were treated with cycloheximide several hours before IGF-I stimulation to inhibit the presence of the protein in internal cell membranes.

Polarization and chemotactic analysis of membrane-cholesterol-depleted cells

Serum-starved MCF-7 cells seeded on vitronectin-coated slides were incubated with 10 mM cyclodextrin (CD) (30 min at 37°C). Under these conditions, CD treatment does not induce cell detachment from the substrate or modify cell viability (data not shown). After this incubation, CD was removed by repeated washing with serum-free MEM with 0.01% BSA (MEM–BSA), then stained with filipin as described (Keller and Simons, 1998). For cholesterol replenishment experiments, CD-treated cells were incubated (30 min at 37°C) in medium containing 2 μg/ml of free cholesterol; cholesterol was subsequently removed by washing with MEM–BSA and cells were stained with filipin.

For chemotaxis, MCF-7 cells were trypsinized, resuspended in MEM–BSA, then treated with CD or CD plus cholesterol, as described above. In all cases, 10^5 cells in MEM–BSA were seeded in the upper chamber of vitronectin-coated transwells (Costar, Cambridge, MA). Lower chambers were filled with MEM–BSA containing IGF-I at 1 ng/ml; after 8 h of incubation at 37°C, transwells were disassembled and the cells on the lower surface stained. Cell numbers were calculated as described previously (Mira *et al*., 1999).

IGF-1R-mediated signaling pathway of membrane-cholesterol-depleted cells

MCF-7 cells plated on vitronectin were depleted of membrane cholesterol and replenished with free cholesterol as described above. These cells were serum starved and some were IGF-I stimulated for various times at 37°C. Cells were subsequently lysed with RIPA buffer (20 mM Tris–HCl pH 8.0, 137 mM NaCl, 1 mM $MgCl_2$, 1 mM $CaCl_2$, 10% glycerol, 1% NP-40, 0.5% deoxycholate, 0.1% SDS) supplemented with a protease and phosphatase inhibitor cocktail. Normalized protein amounts for each fraction were analyzed by SDS–PAGE and Western blotting with anti-PY, anti-IGF-1R β-subunit and anti-insulin receptor substrate-1 (IRS-1) antibodies. Densitometric analysis of digitalized blots was performed with NIH Image software on a Macintosh computer.

Triton X-100 flotation experiments

For analysis of detergent-insoluble complexes in flotation gradients, non-transfected, and GFP-, GFP-GPI-, GFP-ephrinB1wt- or GFP-ephrinB1ΔC-transfected MCF-7 cells were plated on 6-cm vitronectin-coated culture dishes and depleted in serum-free medium, several hours before IGF-I treatment. Plates were cooled on ice, washed with phosphate-buffered saline (PBS) and scraped in 300 μl of TXNE buffer (50 mM Tris–HCl pH 7.4, 150 mM NaCl, 5 mM EDTA, 0.2% Triton X-100) containing a protease and phosphatase inhibitor cocktail. Cells were then extracted for 20 min on ice and the extract subsequently brought to 35% Optiprep. One-third of the lysate was sequentially overlayered with 3.5 ml of 30% Optiprep in TXNE and 200 of μl TXNE in an SW60 tube. After centrifugation (170 000 *g* for 4 h at 4°C), five fractions were collected from the top to the bottom of the gradient and precipitated with trichloroacetic acid. Normalized protein amounts for each fraction were analyzed by SDS–PAGE and Western blotting. Cholesterol depletion experiments were performed as above.

Immunofluorescence and antibody-induced patching

For CCR5 detection by immunofluorescence, cells were trypsinized and plated on vitronectin-coated 8-well-chamber glass slides. Cells were fixed for 5 min on ice with 3.7% paraformaldehyde in PBS, washed in PBS with 2 mg/ml BSA (PBS–BSA), then permeabilized for 10 min with methanol at –20°C. The fixed and permeabilized cells were blocked with 5% goat serum in PBS and incubated (1 h, 4°C) with the antibody dilution in PBS with 1% goat serum. Finally, samples were incubated with the appropriate Cy3-conjugated secondary antibody under the same conditions. Slides were mounted in Vectashield medium containing DAPI (Vector Laboratories, Burlingame, CA). When paxillin and GFP-tagged proteins were detected, the permeabilization step with methanol was replaced by cell incubation with 0.1% Triton X-100 in PBS (10 min at 4°C).

For antibody-mediated lateral cross-linking, cells were incubated (30 min at 12°C) with antibody to IGF-1R, TfR or a polyclonal anti-HA to patch ephrinB1wt and ephrinB1ΔC, then washed at 4°C in PBS–BSA. Further cross-linking was performed with a Cy3 second antibody (30 min at 12°C). At this temperature, internalization of antibody–receptor complexes was not observed. Cells were fixed and mounted as described above. TfR were also visualized by incubating MCF-7 cells with rhodamine-labeled human transferrin (Molecular Probes, Eugene, OR) for 30 min at 37°C; cells were then washed extensively and fixed with paraformaldehyde.

In all cases, cells were visualized by confocal laser scanning microscopy (Leica, Cambridge, UK). When two colors were used, the linear signal intensities detected for both fluorophors were covered by a linear scale of pixel intensities. Digital images were processed using Photoshop software (Adobe Systems, Mountain View, CA). To improve visualization, images showing a single color channel were in some cases transferred to a gray scale.

FITC–CTx labeling and co-patching experiments

Cells were fixed with 1% paraformaldehyde for 5 min on ice, then incubated with FITC–CTx (6 μg/ml) and either anti-CCR5 or anti-IGF-I (KM5A1) antibody for 30 min in PBS–BSA. Cy3-labeled second antibody was added and incubated for 30 min. Finally, cells were incubated with methanol at –20°C for 10 min and mounted as above.

For co-patching experiments, unfixed cells were incubated with FITC–CTx plus either anti-TfR or anti-IGF-1R (α-IR3) at 12°C for 30 min. Primary antibodies were further clustered by adding Cy3-labeled secondary antibody in the same incubation conditions. Finally, cells were fixed by incubating them for 5 min with 3.7% paraformaldehyde at 4°C and for an additional 10 min with methanol at –20°C before mounting as above. Cells were visualized by confocal laser scanning microscopy.

Acknowledgements

We would like to thank Drs F.Sánchez-Madrid and P.Scheiffele for critical reading of the manuscript, and Drs M.Mellado and J.M.R.Frade for the gift of CCR5-02 antibody. This work was partially supported by grants from the Spanish CICyT/EU and the CAM, and from Pharmacia & Upjohn. The Department of Immunology and Oncology was founded and is supported by the Spanish Research Council (CSIC) and Pharmacia & Upjohn.

References

Allen,W., Zicha,D., Ridley,A. and Jones,G. (1998) A role for Cdc42 in macrophage chemotaxis. *J. Cell Biol.*, **141**, 1147–1157.

Bailly,M., Yan,L., Whitesides,G., Condeelis,J. and Segall,J. (1998) Regulation of protrusion shape and adhesion to the substratum during chemotactic responses of mammalian carcinoma cells. *Exp. Cell Res.*, **241**, 285–299.

Bretscher,M. and Aguado-Velasco,C. (1998) Membrane traffic during cell locomotion. *Curr. Opin. Cell Biol.*, **10**, 537–541.

Brown,D. and Rose,J. (1992) Sorting of GPI-anchored proteins to glycolipid-enriched membrane subdomains during transport to the apical cell surface. *Cell*, **68**, 533–544.

Brückner,K., Labrador,J., Scheiffele,P., Herb,A., Seeburg,P. and Klein,R. (1999) EphrinB ligands recruit GRIP family PDZ adaptor proteins into raft membrane microdomains. *Neuron*, **22**, 511–524.

Doerr,M. and Jones,J. (1996) The roles of integrins and extracellular matrix proteins in the insulin-like growth factor I-stimulated chemotaxis of human breast cancer cells. *J. Biol. Chem.*, **271**, 2443–2447.

Dotti,C. and Simons,K. (1990) Polarized sorting of viral glycoproteins to the axon and dendrites of hippocampal neurons in culture. *Cell*, **62**, 63–72.

Friedrichson,T. and Kurzchalia,T. (1998) Microdomains of GPI-anchored proteins in living cells revealed by crosslinking. *Nature*, **394**, 802–805.

Gingras,D., Gauthier,F., Lamy,S., Desrosiers,R. and Beliveau,R. (1998) Localization of RhoA GTPase to endothelial caveolae-enriched membrane domains. *Biochem. Biophys. Res. Commun.*, **247**, 888–893.

Harder,T. and Simons,K. (1999) Clusters of glycolipid and glycosylphosphatidylinositol-anchored proteins in lymphoid cells: accumulation of actin regulated by tyrosine phosphorylation. *Eur. J. Immunol.*, **29**, 556–562.

Harder,T., Scheiffele,P., Verkade,P. and Simons,K. (1998) Lipid domain structure of the plasma membrane revealed by patching of membrane components. *J. Cell Biol.*, **141**, 929–942.

Hopkins,C., Gibson,A., Shipman,M., Strickland,D. and Trowbridge,I. (1994) In migrating fibroblasts, recycling receptors are concentrated in narrow tubules in the pericentriolar area, and then routed to the plasma membrane of the leading lamella. *J. Cell Biol.*, **125**, 1265–1274.

Izzard,C. and Lochner,L. (1980) Formation of cell-to-substrate contacts during fibroblast motility: an interference-reflexion study. *J. Cell Sci.*, **42**, 81–116.

Keller,P. and Simons,K. (1998) Cholesterol is required for surface transport of influenza virus hemagglutinin. *J. Cell Biol.*, **140**, 1357–1367.

Lauffenburger,D. and Horwitz,A. (1996) Cell migration: a physically integrated molecular process. *Cell*, **84**, 359–369.

Lawson,M. and Maxfield,F. (1995) Ca^{2+} and calcineurin-dependent recycling of an integrin to the front of migrating neutrophils. *Nature*, **377**, 75–79.

Ledesma,M., Simons,K. and Dotti,C. (1998) Neuronal polarity: essential role of protein–lipid complexes in axonal sorting. *Proc. Natl Acad. Sci. USA*, **95**, 3966–3971.

Ledesma,M., Brügger,B., Bünning,C., Wieland,F. and Dotti,C. (1999) Maturation of the axonal plasma membrane requires upregulation of sphingomyelin synthesis and formation of protein–lipid complexes. *EMBO J.*, **18**, 1761–1771.

Mañes,S., Kremer,L., Albar,J., Mark,C., Llopis,R. and Martínez-A,C. (1997) Functional epitope mapping of insulin-like growth factor I (IGF-I) by anti-IGF-I monoclonal antibodies. *Endocrinology*, **138**, 905–915.

Mañes,S., Mira,E., Gómez-Moutón,C., Zhao,Z., Lacalle,R. and Martínez-A,C. (1999) Concerted activity of tyrosine phosphatase SHP-2 and focal adhesion kinase in regulation of cell motility. *Mol. Cell. Biol.*, **19**, 3125–3135.

McKay,D., Kusel,J. and Wilkinson,P. (1991) Studies of chemotactic factor-induced polarity in human neutrophils. Lipid mobility, receptor redistribution and the time-sequence of polarization. *J. Cell Sci.*, **100**, 473–479.

Meili,R., Ellsworth,C., Lee,S., Reddy,T., Ma,H. and Firtel,R. (1999) Chemoattractant-mediated transient activation and membrane localization of Akt/PKB is required for efficient chemotaxis to cAMP in *Dictyostelium*. *EMBO J.*, **18**, 2092–2105.

Merrit,E., Sarfaty,S., van den Akker,F., L'Hoir,C., Martial,J. and Hol,W. (1994) Crystal structure of cholera toxin B-pentamer bound to receptor GM1 pentasaccharide. *Protein Sci.*, **3**, 166–175.

Mira,E., Mañes,S., Lacalle,R., Márquez,G. and Martínez-A,C. (1999) IGF-I-triggered cell migration and invasion are mediated by the matrix metalloproteinase MMP-9. *Endocrinology*, **140**, 1657–1664.

Montixi,C., Langlet,C., Bernard,A., Thimonier,J., Dubois,C., Wurbel,M., Chauvin,J., Pierres,M. and He,H. (1998) Engagement of T cell receptor triggers its recruitment to low-density detergent-insoluble membrane domains. *EMBO J.*, **17**, 5334–5348.

Müsch,A., Xu,H., Shields,D. and Rodriguez-Boulan,E. (1996) Transport of vesicular stomatitis virus to the cell surface is signal mediated in polarized and nonpolarized cells. *J. Cell Biol.*, **133**, 543–558.

Nieto,M., Frade,J., Sancho,D., Mellado,M., Martínez-A,C. and Sánchez-Madrid,F. (1997) Polarization of chemokine receptors to the leading edge during lymphocyte chemotaxis. *J. Exp. Med.*, **186**, 153–158.

Nobes,C. and Hall,A. (1999) Rho GTPases control polarity, protrusion, and adhesion during cell movement. *J. Cell Biol.*, **144**, 1235–1244.

Oliferenko,S., Paiha,K., Harder,T., Gerke,V., Schwärzler,C., Schwarz,H., Beug,H., Günthert,U. and Huber,L. (1999) Analysis of CD44-containing lipid rafts: recruitment of annexin II and stabilization by the actin cytoskeleton. *J. Cell Biol.*, **146**, 843–854.

Parent,C., Blacklock,B., Froehlich,W., Murphy,D. and Devreotes,P. (1998) G protein signaling events are activated at the leading edge of chemotactic cells. *Cell*, **95**, 81–91.

Regen,C. and Horwitz,A. (1992) Dynamics of β1 integrin-mediated adhesive contacts in motile fibroblasts. *J. Cell Biol.*, **119**, 1347–1359.

Rohlik,Q., Adams,D., Kull,F. and Jacobs,S. (1987) An antibody to the receptor for insulin-like growth factor I inhibits the growth of MCF-7 cells in tissue culture. *Biochem. Biophys. Res. Commun.*, **149**, 276–281.

Scheiffele,P., Roth,M.G. and Simons,K. (1997) Interaction of influenza virus haemagglutinin with sphingolipid-cholesterol membrane domains via its transmembrane domain. *EMBO J.*, **16**, 5501–5508.

Schmidt,C., Horwitz,A., Lauffenburger,D. and Sheetz,M. (1993) Integrin-cytoskeletal interactions in migrating fibroblasts are dynamic, asymmetric, and regulated. *J. Cell Biol.*, **123**, 977–991.

Schmitt,M. and Bultmann,B. (1990) Fluorescent chemotactic peptide as tools to identify the f-Met-Leu-Phe receptor on human granulocytes. *Biochem. Soc. Trans.*, **18**, 219–222.

Schon,A. and Freire,E. (1989) Thermodynamics of intersubunit interactions in cholera toxin upon binding to the oligosaccharide portion of its cell surface receptor, ganglioside GM1. *Biochemistry*, **28**, 5019–5024.

Servant,G., Weiner,O., Neptune,E., Sedat,J. and Bourne,H. (1999) Dynamics of a chemoattractant receptor in living neutrophils during chemotaxis. *Mol. Biol. Cell*, **10**, 1163–1178.

Simons,K. and Ikonen,E. (1997) Functional rafts in cell membranes. *Nature*, **387**, 569–572.

Simons,K. and Wandinger-Ness,A. (1990) Polarized sorting in epithelia. *Cell*, **62**, 207–210.

Simons,M., Keller,P., De Strooper,B., Beyreuther,K., Dotti,C. and Simons,K. (1998) Cholesterol depletion inhibits the generation of β-amyloid in hippocampal neurons. *Proc. Natl Acad. Sci. USA*, **95**, 6460–6464.

Spiegel,S., Kassis,S., Wilchek,M. and Fishman,P. (1984) Direct visualization of redistribution and capping of fluorescent gangliosides on lymphocytes. *J. Cell Biol.*, **99**, 1575–1581.

Stauffer,T. and Meyer,T. (1997) Compartmentalized IgE receptor-mediated signal transduction in living cells. *J. Cell Biol.*, **139**, 1447–1454.

Stowers,L., Yelon,D., Berg,L. and Chant,J. (1995) Regulation of the polarization of T cells toward antigen-presenting cells by Ras-related small GTPase Cdc42. *Proc. Natl Acad. Sci. USA*, **92**, 5027–5031.

Sullivan,S., Daukas,G. and Zigmond,S. (1984) Asymmetric distribution of chemotactic peptide receptor on polymorphonuclear leukocytes. *J. Cell Biol.*, **99**, 1461–1467.

Taylor,R., Duffus,W., Raff,M. and de Petris,S. (1971) Redistribution and pinocytosis of lymphocyte surface immunoglobulin molecules induced by anti-immunoglobulin antibody. *Nature New Biol.*, **233**, 225–229.

Varma,R. and Mayor,S. (1998) GPI-anchored proteins are organized in submicron domains at the cell surface. *Nature*, **394**, 798–801.

Vicente-Manzanares,M., Montoya,M., Mellado,M., Frade,J., del Pozo,M., Nieto,M., de Landazuri,M., Martínez-A,C. and Sánchez-Madrid,F. (1998) The chemokine SDF-1α triggers a chemotactic response and induces cell polarization in human B lymphocytes. *Eur. J. Immunol.*, **28**, 2197–2207.

Viola,A., Schroeder,S., Sakakibara,Y. and Lanzavecchia,A. (1999) T lymphocyte costimulation mediated by reorganization of membrane microdomains. *Science*, **283**, 680–682.

Walter,R. and Marasco,W. (1984) Localization of chemotactic peptide receptors on rabbit neutrophils. *Exp. Cell Res.*, **154**, 613–618.

Xavier,R., Brennan,T., Li,Q., McCormack,C. and Seed,B. (1998) Membrane compartmentalization is required for efficient T cell activation. *Immunity*, **8**, 723–732.

Xiao,Z., Zhang,N., Murphy,D. and Devreotes,P. (1997) Dynamic distribution of chemoattractant receptors in living cells during chemotaxis and persistent stimulation. *J. Cell Biol.*, **139**, 365–374.

Yoshimori,T., Keller,P., Roth,M. and Simons,K. (1996) Different biosynthetic transport routes to the plasma membrane in BHK and CHO cells. *J. Cell Biol.*, **133**, 247–256.

Zigmond,S. (1974) Mechanisms of sensing chemical gradients by polymorphonuclear leukocytes. *Nature*, **249**, 450–452.

Zigmond,S. (1977) Ability of polymorphonuclear leukocytes to orient in gradients of chemotactic factors. *J. Cell Biol.*, **75**, 606–616.

Received June 22, 1999; revised and accepted September 24, 1999